Earth and Planetary Science Letters 576 (2021) 117217

Contents lists available at ScienceDirect

Earth and Planetary Science Letters

www.elsevier.com/locate/epsl

ENSO, sun and megadroughts in SW USA during the last 11,000 years

Gonzalo Jiménez-Moreno [a,*], R. Scott Anderson [b], Jacqueline J. Shinker [c]

[a] Departamento de Estratigrafía y Paleontología, Universidad de Granada, Fuente Nueva s/n, 18002, Granada, Spain
[b] School of Earth & Sustainability, Northern Arizona University, Flagstaff, AZ 86011, USA
[c] Department of Geology and Geophysics, University of Wyoming, Laramie, WY 82071, USA

ARTICLE INFO

Article history:
Received 9 April 2021
Received in revised form 30 July 2021
Accepted 17 September 2021
Available online 1 October 2021
Editor: Y. Asmerom

Keywords:
P. edulis
Holocene
ENSO
solar activity
Southern Rocky Mountains
USA

ABSTRACT

El Niño Southern Oscillation (ENSO) is one of the most important modes of variability in the climate system. However, ENSO instrumental records are too short to characterize its natural variability at long-term timescales. Paleoclimate records showing ENSO variability during the Holocene on centennial and millennial timescales are rare but critical for our understanding of long-term multidecadal- to millennial-scale variability. Here we used several climate sensitive piñon pine (*Pinus edulis*) pollen records from the Southern Rockies, USA, to produce a detailed continuous record of effective precipitation and ENSO-like variability for the last 11,000 yrs. La Niña conditions dominated the Early Holocene while El Niño conditions enhanced in an increasing trend over the last 6,000 yrs. This trend was modulated by millennial-scale and ENSO-like hydrological activity at prominent 900-1,000-yr cycles and the amplitude of these cycles increased until present. Enhanced La Niña and related multidecadal megadroughts occurred in the Southern Rockies centered at ca. 10, 8, 6.8, 5.8, 4.8, 4, 3, 2.2, 1 ka. Insolation and solar output changes are suggested here as the main triggers for ENSO climate and vegetation changes. Our analysis of recent strong La Niña events, representing modern climate analogs of past conditions, indicates anomalously dry conditions persisting annually, leading to prolonged drought that impact piñon pine growth. Following the thermostat hypothesis and the Sun-ENSO link, such dry conditions are expected to prevail in the future, which combined with increasing temperatures, will most likely generate megadroughts in the SW USA.

1. Introduction

ENSO is a mode of variability representing interannual changes in sea-surface temperatures, conditioning atmospheric circulation across the equatorial Pacific Ocean (Cane, 2005). Instrumental records show that ENSO alternates between anomalously warm (El Niño); anomalously cold (La Niña) conditions; and neutral conditions in the tropical Pacific at intervals of 2–8 yrs (Cane, 2005). This sea-surface temperature anomaly produces atmospheric teleconnections that influence climate in many regions of the world (Cane, 2005, Taschetto et al., 2021). Tropical deep convection significantly alters the position of the jet stream and thus storm systems, impacting western US precipitation (Fig. 1, Yeh et al., 2018, Taschetto et al., 2021). During El Niño events, anomalously warm SSTs in the tropical eastern Pacific shift deep convection eastwards and the jet stream over the Pacific becomes less wavy and splits into a strong subtropical jet stream near the equator and a weaker polar jet stream (Fig. 1A). In the Southern Rockies and southwest (SW) regions of North America, El Niño events are associated with above-average precipitation (Shinker and Bartlein, 2009, Taschetto et al., 2021). La Niña events are associated with below-average precipitation and drought as the jet stream curves and shifts north, diverting storms and precipitation away from the region (Cook et al., 2007, Conroy et al., 2009, Arriaga-Ramírez and Cavazos, 2010, Heyer et al., 2017, Fig. 1B). In addition, anomalously cold temperatures tend to occur in the Southern Rockies during El Niño years, especially in summer (Heyer et al., 2017). On the other hand, above average temperatures occur throughout most of the year during the La Niña years in the study area (Heyer et al., 2017, https://www.psl.noaa.gov/enso/climaterisks/).

Even though the instrumental record suggests ENSO is modulated at low frequencies (Taschetto et al., 2021), paleoclimate reconstructions show that ENSO has changed at decadal- centennial- and millennial-scales, but only a few rare records show long-term ENSO variability during the Holocene (Rodó and Rodriguez-Arias, 2004, Rein et al., 2005, Conroy et al., 2008, Emile-Geay et al., 2013, 2021). Therefore, a better understanding of past climate variability at centennial- and millennial-scales is crucial to our understanding of natural climate variability upon which anthropogenic

* Corresponding author.
E-mail address: gonzaloj@ugr.es (G. Jiménez-Moreno).

https://doi.org/10.1016/j.epsl.2021.117217

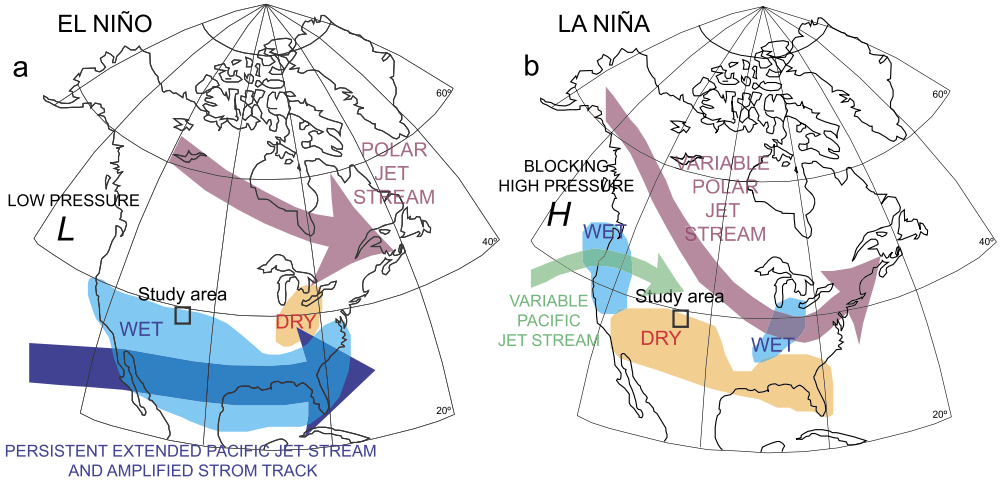

Fig. 1. Maps of study area. (A) Map of North America showing general atmospheric patterns and precipitation including the location of the studied sites during El Niño conditions and (B) during La Niña conditions. Modified from https://www.climate.gov/news-features/blogs/enso/united-states-el-ni~{n}o-impacts-0 and https://www.pmel.noaa.gov/elnino/lanina-faq.

climate change is superimposed. Of special interest are those effects on arid regions, such as the SW USA, whose populations and economies are vulnerable to variable precipitation regime (Cook et al., 2007).

Previous studies suggest that ENSO's evolution through time was due to external forcing factors such as changes in Earth's orbit and insolation, solar activity or in the atmospheric greenhouse gas composition (Emile-Geay et al., 2021). Orbital-scale changes in insolation are the major forcing mechanism regulating climate and evapotranspiration at long-term (i.e., glacial-interglacial cycles, Rein et al., 2005) timescales, and variations in ENSO have been suggested as the major trigger for shorter centennial-scale precipitation shifts in SW USA and many regions of the world during the Holocene (Conroy et al., 2009, Arriaga-Ramírez and Cavazos, 2010, Barron and Anderson, 2011). However, little is known about the fundamental forcing mechanism triggering millennial- and centennial-scale ENSO climate variability while some previous studies point to solar activity changes affecting sea-surface temperatures (Mann et al., 2009) or periodic movement of the Intertropical Convergence Zone (ITCZ, Haug et al., 2001).

Moisture availability has played a dominant role in the past population dynamics of *P. edulis* woodlands of western USA (Swetnam and Betancourt, 1998, Woodhouse, 2003, Clifford et al., 2013, see present-day distribution in Fig. S1). Winter minimum precipitation is known to be significant in limiting modern *P. edulis* today (Cole et al., 2008), as shown by recent studies documenting widespread *P. edulis* die-off that occurred after extensive La Niña-related drought in the SW USA during the early 2000s (Allen and Breshears, 1998, Breshears et al., 2005, Anderson and Feiler, 2009, Clifford et al., 2013). This suggests that a combination of drought and high temperatures (previously defined as 'global-change-type drought'), climate conditions that occur during persistent La Niña conditions in the study area (Heyer et al., 2017, https://www.psl.noaa.gov/enso/climaterisks/), can be lethal for tree species such as *P. edulis* (Breshears et al., 2005, Clifford et al., 2013).

Previous pollen studies from the Southern Rockies have documented increases and expansion of *P. edulis*, mostly during the Middle and Late Holocene, suggesting a relationship with increased ENSO winter precipitation there (Anderson and Feiler, 2009, Jiménez-Moreno and Anderson, 2012). However, a direct comparison between *P. edulis* occurrence and ENSO was never explored, and thus a clear relationship was never confirmed. Our analysis of the Middle to Late Holocene *P. edulis* pollen record shows a strong correlation with ENSO-like conditions at short, centennial and millennial scales.

2. Materials and methods

A hydrologically sensitive *P. edulis* stack for the last 11,000 cal yr BP (Fig. 2) was obtained using seven detailed pollen records (sample resolution range between 44-250-yrs) from sites within the Colorado and New Mexico Rocky Mountains (Fig. S1; Table S1). We used published original data of absolute chronologies for the individual sites (Figure S2). The studied sites are located at high elevation between 2700-3667 m and latitudes ranging from 35-40°N. *P. edulis* abundance data were resampled (linear interpolation) at 100-yr windows using Analyseries (Supplementary Information), normalized to stabilize the variance, and standardized to make them comparable and to minimize the local differences within sites and the error of individual site chronologies. To do that we used the method applied by Power et al. (2008) (Supplementary Information). *P. edulis* from individual records show similar trends at multi-millennial scales and thus positive correlation ($r = 0.38$–0.79, $p < 0.0001$; mean r value $= 0.63$; Table S2). The *P. edulis* stack was calculated using the median of individual site z-score values (Figs. S2 and S3). A more detailed 50-yr resolution *P. edulis* stack was also obtained for the last 1,250 cal yr BP following the same methodology but only applied to the higher-resolution 4 sites (Stewart Lake, Kite Lake, Tiago Lake and Chihuahueños Bog; resolution $\sim$ 33-46 yrs between pollen samples).

To explore a *P. edulis*-ENSO-Sun relationship a visual and statistical correlation was performed between the *P. edulis* stack, well-known ENSO-proxy and paleohydrological records and solar activity $\Delta^{14}C$ nuclide production rates (Reimer et al., 2020) for the past 11,000 yrs from the study area (Fig. 2; Tables S3 and S4). A more detailed comparison was also performed between a higher resolution (50-yr) *P. edulis* paleohydrological stack, $\Delta^{14}C$ solar activity (Reimer et al., 2020) and tree-ring-based precipitation reconstruction for the western USA (Cook et al., 2004) for the last 1200 cal yr BP (Fig. 4).

To explore the climate mechanisms associated with dry conditions impacting *P. edulis* in the southern Rocky Mountains, a modern climate analog approach was used. The modern climate analog approach provides process-based examples of how climate mechanisms, associated with prolonged or extreme conditions (e.g. drought associated with strong La Niñas), can influence hydroclimatic extremes seen in the paleoenvironmental record (e.g., reduced *P. edulis* as reconstructed through sedimentary pollen, see also Mock and Brunelle-Daines, 1999, Edwards et al., 2001, Shinker et al., 2006, Mock and Shinker, 2013, Shinker, 2014, Carter et al., 2018a, 2018b). Modern examples of strong La Niña conditions are

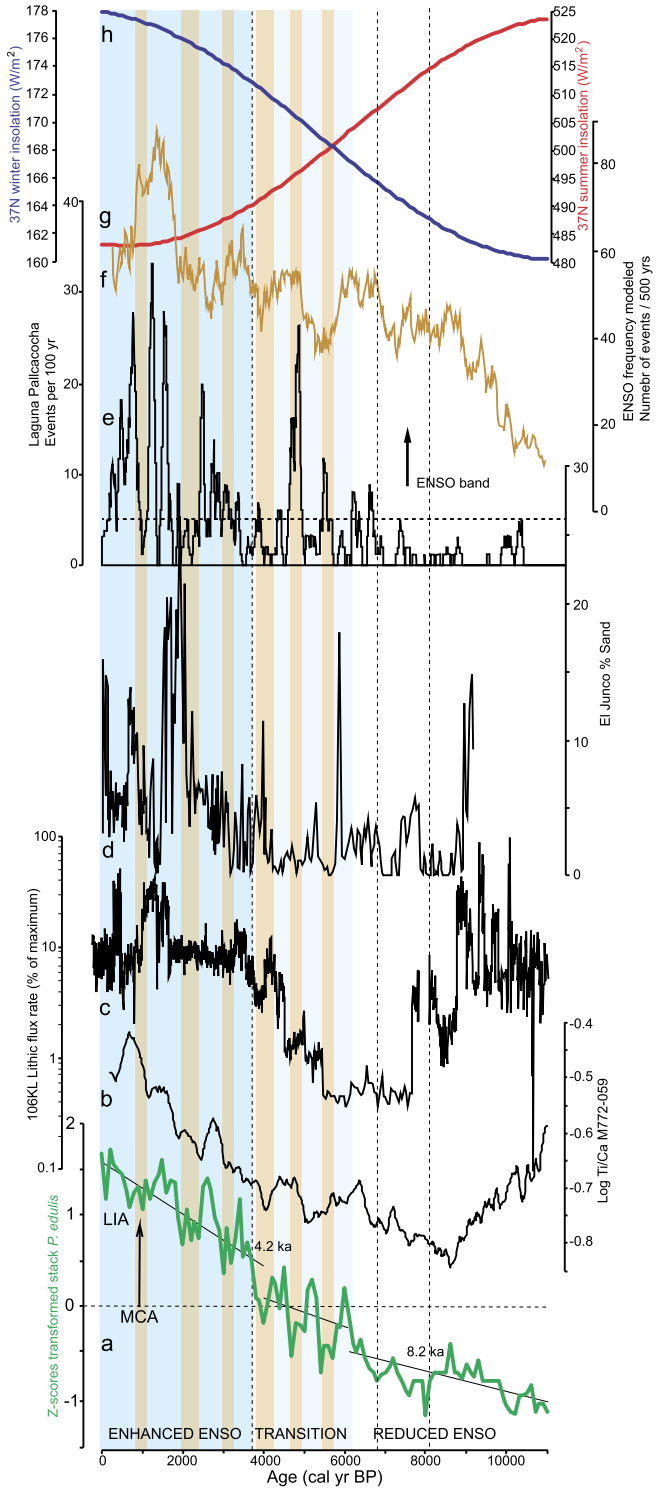

Fig. 2. Holocene time series of *P. edulis* stack, ENSO and insolation. (A) *P. edulis* stack time series showing trend lines. (B) Seven point-smoothing of Log Ti/Ca ratios from M772-059 riverine runoff record from the coast off Peru (Mollier-Vogel et al., 2013). (C) Lithic flux record from 106KL core off Peru (Rein et al., 2005). (D) El Junco lake sediment record in Ecuador (Conroy et al., 2008). (E) clastic record from Laguna Pallcacocha in Ecuador (Rodó and Rodriguez-Arias, 2004). (F) Modeled ENSO frequency during the Holocene (Clement et al., 2000). (G) and (H), Summer and Winter insolation for 37°N (Laskar et al., 2004). Well known climatic events are marked: 8.2 ka, 4.2 ka, MCA (Medieval Climate Anomaly) and LIA (Little Ice Age). Light and dark blue shading indicate transitional (i.e., moderate values of *P. edulis*, with peaks over 0) and enhanced (i.e., all values of *P. edulis* over 0) ENSO during the Holocene. Orange shading shows suggested centennial-scale cyclical megadroughts in southwestern North America based on *P. edulis* stack. (For interpretation of the colors in the figure(s), the reader is referred to the web version of this article.)

known to persist across multiple seasons in the southern Rocky Mountains and SW (Cook et al., 2007, Conroy et al., 2009, Arriaga-Ramírez and Cavazos, 2010), with statistically significant negative hydroclimate impacts (Heyer et al., 2017). Such conditions (strong La Niña events) are used here as an analog to assess not just the climatic state of dry conditions (e.g. as evident in the paleoenvironmental record), but the climate mechanisms such as atmospheric motion and moisture availability (not evident in the paleoenvironmental record) that can lead to and influence prolonged drought in the region. Therefore, we use the modern climate analog approach here as an additional example of how mechanisms associated with hydroclimatic drought impacts vegetation changes in the southern Rocky Mountains.

To assess the teleconnections between La Niña and the study region we analyzed strong to moderately strong La Niña conditions (1988/1989; 1998/1999; 1999/2000) identified from the Oceanic Niño Index (ONI), representing SST anomalies in the Niño 3.4 region (5°N-5°S, 120°-170°W, Carter et al., 2018b). We used atmospheric and surface climate variables from the North American Regional Reanalysis dataset (Mesinger et al., 2006, a 32-km gridded dataset) to calculate and map anomalous patterns based on selected La Niña conditions (Fig. S6). The atmospheric variables were used to represent atmospheric pressure and motion in the mid-troposphere (500 mb geopotential height); moisture availability in the atmosphere (850 mb specific humidity); and information related to rising (enhances precipitation) or sinking motions (suppresses precipitation) in the atmosphere (500 mb omega). The surface climate variables used, precipitation rate at the surface, surface temperature and soil moisture, represent surface processes relevant to *P. edulis* growth. We focus on the anomalous conditions annually for our selected case years because *P. edulis* growth is most negatively impacted by persistent dry hydroclimatic conditions across multiple seasons and multiple years. The composite-anomaly values were calculated for each year by averaging (compositing) the selected La Niña case years and comparing that composite value to the long-term mean (1981-2010). The resulting composite-anomaly values were mapped to identify atmospheric and surface conditions during selected La Niña cases. To illustrate the large spatial scales at which atmospheric variables operate we mapped such variables at a continental scale, while small scale processes, such as precipitation and soil moisture were mapped at a regional scale to align our climate analyses with regional *P. edulis* patterns.

3. Results

In this study we show that Holocene records of *P. edulis* from the Southern Rockies of New Mexico and Colorado display significant covariation over multimillennial-scales, documenting increasing importance of the tree over the last 6,000 yrs, concurrent with short-term, centennial- and millennial-scale variability (Fig. S2; correlation between records shown in Table S2). These variations are diagnostic of a common paleoenvironmental and paleoclimatic control of this tree species population. Therefore, to build a regional *P. edulis* record we synthesized seven published pollen records into a *P. edulis* stack, which shows a long-term trend from low values and lower amplitude variability in the Early and early-Middle Holocene until ~6,000 cal yr BP, after which, an increasing trend is punctuated by episodic decreases (Fig. 2). A similar long-term pattern of change is shown by ENSO records from the equatorial Pacific area (Rodó and Rodriguez-Arias, 2004, Rein et al., 2005, Mollier-Vogel et al., 2013) and their comparison with the *P. edulis* stack shows strong statistical correlations (Fig. 2; correlation between records shown in Tables S3 and S4).

The individual *P. edulis* records and thus the *P. edulis* stack also show millennial- and centennial-scale climate variability superim-

posed on the general trends in the last 11,000 cal yr BP (Figs. 2 and 3). Studied detrended records of *P. edulis* generally show covariation at millennial-scales with overall positive correlations between them (Table S2). Sites in the southern part of the transect show overall higher correlation than those to the north (Kite and Tiago Lakes; Table S2). This may result from their position at the northern boundary of the core limit of the present-day distribution of *P. edulis* in the area (Tiago Lake; see map in Fig. S1), or the high elevation of the site (Kite Lake at 3667 m), which could have precluded the lake from receiving a strong and significant *P. edulis* pollen signal from the southwest (Tiago) or from lower elevation (Kite) at millennial-scales and represented by low pollen percentages (Fig. S2). In addition, the high elevation of Kite Lake may be buffered from hydroclimatic impacts because of the influence of midlatitude jet stream delivering winter snow and high elevations (Mock, 1996) and prolonged effective moisture at elevation from spring into summer (Shinker and Bartlein, 2010). Additionally, the northerly sites of Tiago and Kite Lakes occur within a transitional region that is minimally impacted by the hydroclimatic influence of ENSO (Wise, 2010, Heyer et al., 2017). However, we opted to keep those two records in the stack to reflect the possible regional heterogeneity and signal of the tail distribution of this taxon in the area as their overall trends remain consistent with the other records in our study.

Visual as well as wavelet and spectral analyses of the *P. edulis* stack show a 900-1000-yr cyclicity that becomes more significant and amplifies in the last 6,000 cal yr BP evolving from a longer-frequency ~2500-yr cycle in the earlier part of the record (Figs. S4 and S5). Minima in *P. edulis* stack occurred in SW USA centered at ca. 10.0, 8.0, 6.8, 5.8, 4.8, 4.0, 3.0, 2.2, 1.0 ka. The variability observed in the synthetic *P. edulis* pollen stack also closely matches large shifts in the solar activity $\Delta^{14}C$ nuclide production rates (Reimer et al., 2020; Fig. 3), and, as well, significant correlation between *P. edulis* stack and ^{14}C production record of solar activity, especially during the last 6,000 cal yr BP ($r = 0.72$; $p < 0.0001$; 300-yr smoothed and filtered at 950-yr; Table S4), occurs.

A highly significant correspondence between solar output and climate can also be observed between the higher resolution (50-yr) *P. edulis* paleohydrological stack, $\Delta^{14}C$ solar activity (Reimer et al., 2020) ($r = 0.82$, $p < 0.0001$; 100-yr smoothed; Table S4) and tree-ring-based precipitation reconstruction for the western USA (Cook et al., 2004) for the last 1200 cal yr BP, which closely covariates at a ~ 200-yr (Suess) solar cycle (Fig. 4; Fig. S5).

The analysis of strong, to moderately strong La Niña events from the modern record using North American Regional Reanalysis data (NARR, Mesinger et al., 2006, Fig. S6) shows that calculated composite-anomaly values through the selected years provide process-based context for the climate mechanisms that impact moisture delivery and growth for *P. edulis*. Climatically, strong La Niña conditions are associated with greater-than-normal atmospheric pressure persisting through the year (Fig. S6a), with enhanced sinking motions (Fig. S6b). The persistent anomalously strong sinking motions (suppressing precipitation), along with drier-than-normal atmospheric moisture (Fig. S6c), led to persistent lower-than-normal precipitation (Fig. S6d). Tiago and Kite lakes appear slightly wetter than normal, perhaps for the geographic and elevational reasons outlined above. Thus our pollen results are consistent with noted regional ENSO variability. The overall anomalously low precipitation within our study region is further impacted by persistent warmer-than-normal surface temperatures (Fig. S6e), enhancing anomalously dry soil moisture conditions (Fig. S6f) during the years for selected cases.

4. Discussion and conclusions

The biogeographic history of *P. edulis* in the Southwest US documents a widespread distribution at elevations below ~1700 m during the last glacial, between ~40,000 and 11,000 cal yr BP, as clearly documented by abundant packrat midden records (Betancourt et al., 1991, Anderson and Feiler, 2009). This may reflect the abundance of winter-dominated precipitation in the current Sonoran, Chihuahuan and Mojave Deserts, due to southward deflection of the storm track during the LGM, with cold temperatures limiting upslope and northward spread of *P. edulis* during that time. Warmer temperatures during the Early Holocene would have allowed *P. edulis* to slowly spread upslope and northward, but warm and dry conditions during the Early Holocene may have slowed this trend.

Our significant correlation with Holocene ENSO records from the equatorial Pacific area provides strong confirmation that the Holocene *P. edulis* stack mainly reflects a regional hydroclimate signal that could be at least partly related to ENSO variability over southwestern North America, as suggested elsewhere (Anderson and Feiler, 2009, Jiménez-Moreno and Anderson, 2012, Jiménez-Moreno et al., 2019). In this way, low *P. edulis* values during the Early and early-Middle Holocene could reflect reduced ENSO and enhanced La Niña dry conditions precluding moisture-sensitive *P. edulis* woodlands from extensive development in the area. Thus, we conclude that low occurrences of *P. edulis* in its present elevation range within the area was due to extreme cold conditions during the last glaciation and northward migration during the Early Holocene warming being limited by predominant La Niña dry conditions. Our evidence supports the interpretation of weakened ENSO conditions during the Early and Middle Holocene, agreeing with several ENSO proxy records from the eastern Pacific region (Rodó and Rodriguez-Arias, 2004, Rein et al., 2005, Mollier-Vogel et al., 2013), from simple Pacific-only climate models (Clement et al., 2000), and reconstructions of low effective moisture and lake levels in the western USA (Anderson, 1993, Shuman and Marsisek, 2016). Highest summer insolation during the Early Holocene might have also contributed to the low occurrence of *P. edulis*, as evapotranspiration in summer might have been very high. The trend toward increasing *P. edulis* by ~6,000 cal yr BP reflects enhanced effective winter precipitation and soil humidity that could be related to El Niño conditions during the Middle to Late Holocene. This trend, along with the amplitude of the variability, is more pronounced in the last 4,000 cal yr BP (Figs. 2 and 3), which is reflected in additional proxy records and climate simulations (Barron and Anderson, 2011, Koutavas et al., 2006, Liu et al., 2014), in particular in the last 4,000 cal yr BP (Conroy et al., 2008, Koutavas and Joanides, 2012). In order to explain a main climate forcing for the *P. edulis* paleohydrological pattern we follow previous studies that suggest that the observed behavior of ENSO over the Holocene is mostly due to the oceanic, and subsequently atmospheric, response to orbital changes in insolation with changes in the seasonal cycle of solar radiation in the tropics (Clement et al., 2000, Koutavas and Joanides, 2012, Loubere et al., 2013, Fig. 2). Another hypothesis producing the same outcome in terms of enhanced ENSO in the late Middle and Late Holocene is that orbital changes in insolation, with the decrease in summer insolation, triggered a southern displacement of the Intertropical Convergence Zone (ITCZ, Haug et al., 2001, Koutavas et al., 2006). A southward-displaced marine ITCZ would favor less permanent southeast trades, precluding cool upwelling in the eastern tropical Pacific, which via teleconnection in the SW USA would translate in more frequent El Niño conditions (Koutavas et al., 2006, Sulca et al., 2018). Decreasing summer insolation and temperatures during the Middle and Late Holocene (Laskar et al., 2004) would in turn trigger a decline in summer

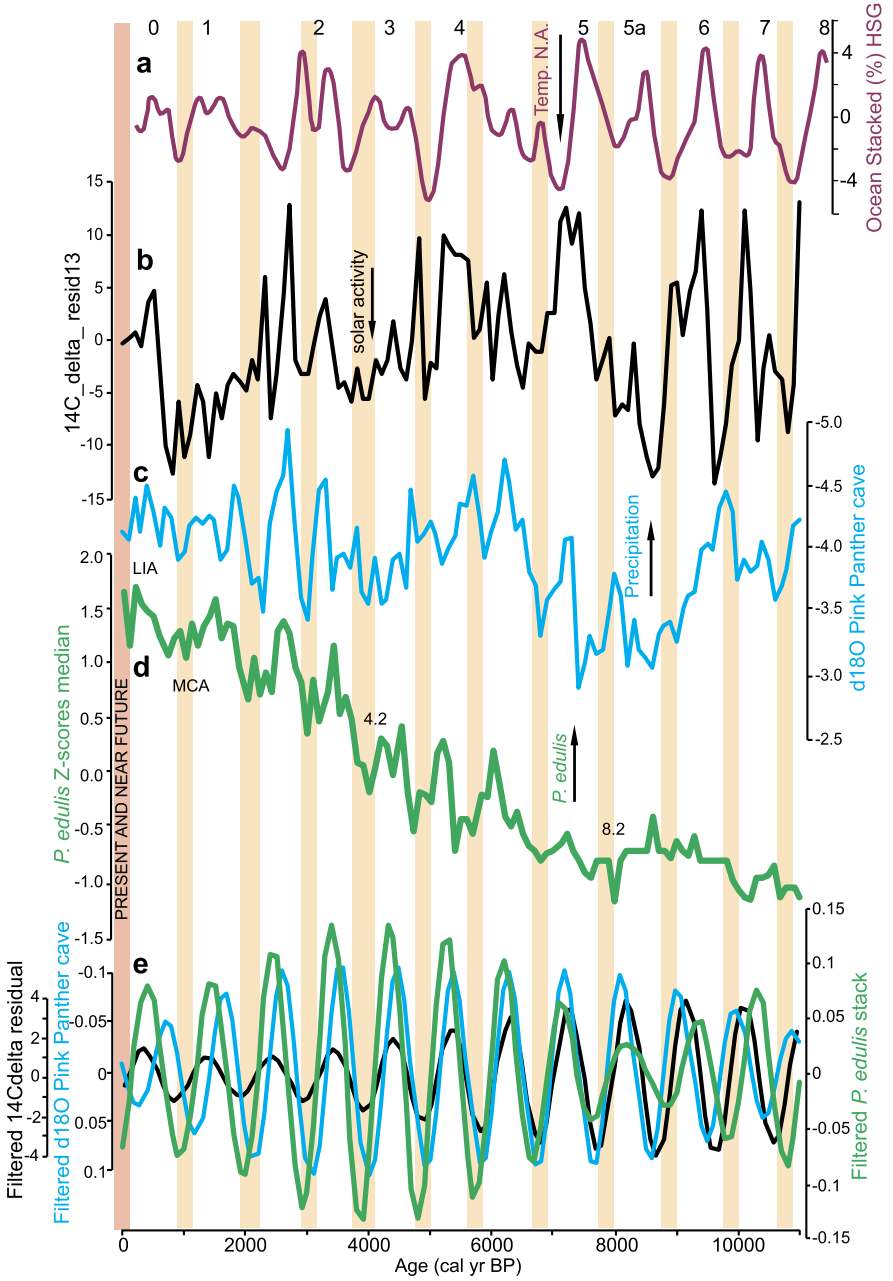

Fig. 3. Holocene ENSO precipitation, solar activity and temperatures from the North Atlantic. (A) stacked marine hematite-stained grains (% HSG) records in percentage from the North Atlantic (Bond et al., 2001). Cold events are marked with numbers from 0 to 8 (Bond et al., 2001). (B) resampled at 100-yr and 29-point smoothed residual Δ14C data calculated from IntCal20 Δ14C (‰) (Reimer et al., 2020). (C) Precipitation $\delta^{18}O$ data from Pink Panther cave, New Mexico (Asmerom et al., 2007). Note that scale is inverted. (D) *P. edulis* stack time series. (E) Comparison between extracted 950-yr waveforms of ENSO *P. edulis* (in green), $\delta^{18}O$ data from Pink Panther cave, New Mexico (Asmerom et al., 2007) (Blue) and solar (Reimer et al., 2020) (black) variability during the Holocene. Centennial-scale 950-yr variability was based on the spectral analysis shown in Figure S4. Note the good covariation between each other. Well known climatic events are marked: 8.2 ka, 4.2 ka, MCA (Medieval Climate Anomaly) and LIA (Little Ice Age). Light and dark blue shading indicate transitional and enhanced ENSO during the Holocene. Orange shading shows suggested centennial-scale cyclical megadroughts in southwestern North America based on the *P. edulis* stack. Following the cyclical pattern in ENSO variability, decadal-scale megadroughts are expected at present and in the next decades in the study area (red shading).

evapotranspiration, producing an increase in soil humidity that *P. edulis* would benefit.

The 900-1000-yr cycle identified in the Holocene *P. edulis* stack is a characteristic pattern of many other Holocene ENSO (Lamy et al., 2001) and paleohydrological records from the study area (Asmerom et al., 2007), providing additional support for the *P. edulis* stack-ENSO link (Fig. S5). Minima in the *P. edulis* stack and thus possibly enhanced La Niña and related multidecadal megadroughts occurred in SW USA centered at ~10,0, 8.0, 6.8, 5.8, 4.8, 4.0, 3.0, 2.2, 1.0 ka. Some of those episodes, in particular the ~8 (8.2 ka), 4 (4.2 ka), and 1 (1.0 ka; Medieval Climate Anomaly, MCA) ka events are, taking into account age uncertainties, well known for extreme aridity in the western USA (Johnson et al., 2013, Calder et al., 2015, Jiménez-Moreno et al., 2019). Significant correlation between the *P. edulis* stack and the ^{14}C production record of solar activity, especially during the last 6,000 cal yr BP ($r = 0.72$; $p < 0.0001$; 300-yr smoothed and filtered at 950-yr; Table S3 and S4), could point to a solar-induced origin of ENSO variability, as the ~1000-yr cycle is one the most pervasive solar cycles over the Holocene (Debret et al., 2009, Fig. 3, Fig. S5), and indeed worldwide (Bond et al., 2001). Although we lack a complete understanding of processes transferring and amplifying small energy variations of solar

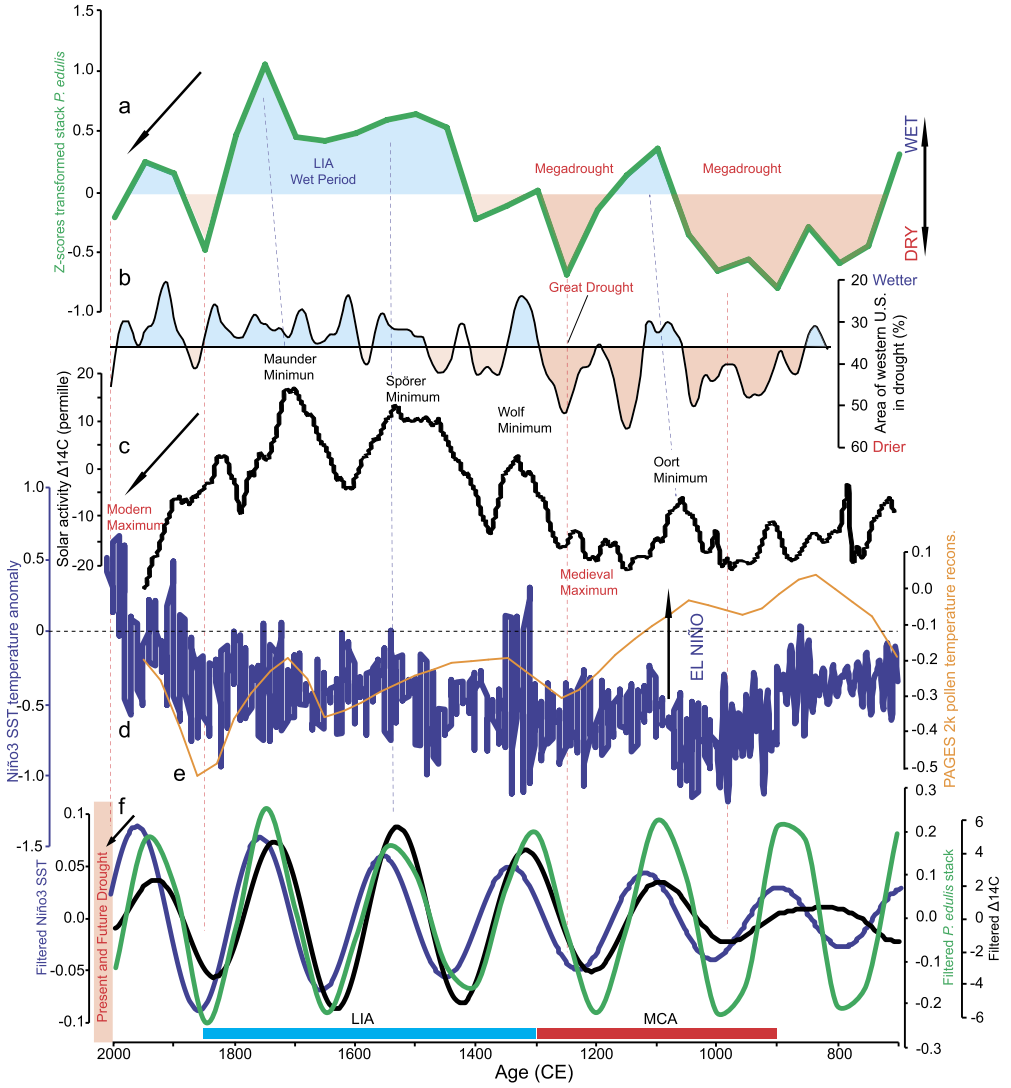

Fig. 4. ENSO reconstruction and solar activity for the last 1300 cal yr BP. (A) *P. edulis* stack at 50-yr resolution for the past 1300 cal yr BP. Red shading indicates dry and blue humid periods. (B) Tree-ring reconstruction of past drought over western North America covering the past 1200 cal yr BP (Cook et al., 2004). Red and blue shading as same as above. (C) Solar activity measured in residual $\Delta^{14}C$ (Reimer et al., 2020). Minima and maxima are indicated. (D) El Niño3 tropical Pacific surface temperature reconstruction (Mann et al., 2009). (E) Pages 2k temperature reconstruction from North America pollen (Pages 2k Consortium, 2013). (F) Gaussian band-pass filtered *P. edulis* stack (Green), El Niño3 SST reconstruction (blue) and solar activity (black) records at 200-yr frequency. Note the covariation of the records at 200-yr cycles. The Medieval Climate Anomaly (MCA; in red) and Little Ice Age (LIA; in blue) periods are shown. Dashed lines show correlations between the *P. edulis* stack, solar activity and Niño3 records. The arrows show the present and near future trend towards La Niña and drought conditions in the study area.

activity to the Earth's surface it seems that variations in solar insolation, amplified by the Bjerknes feedback, conditioned surface water temperatures in the tropical Pacific and atmospheric dynamics and precipitation in the Pacific influence area (ocean thermostat hypothesis, Clement et al., 1996), including the Southern Rockies (Fig. 3). This hypothesis is consistent with previous studies showing a close solar-ENSO relationship at decadal (i.e., 11 yr-cycle, Meehl et al., 2009) and centennial time-scales (Emile-Geay et al., 2013). In addition to anomalously low precipitation, above average temperatures that probably occurred throughout most of the year during the La Niña years in the study area reduced effective moisture, negatively impacting soil moisture and further increasing drought (Heyer et al., 2017). However, climate modeling studies such as the study by Otto-Bliesner et al. (2016) found that a solar-ENSO link is not completely clear, although they did not include in their simulation the "top down" effect of solar variability and thus further studies in this regard need to be accomplished.

Our study suggests that multidecadal-scale La Niña-related megadroughts occurred between 800–1300 CE, consistent with precipitation reconstructions in the western USA (Cook et al., 2004), La Niña–like conditions in the tropical Pacific (Mann et al., 2009), and most likely related to the solar maxima of the Medieval Climate Anomaly (MCA, Reimer et al., 2020) and overall warm temperatures (Pages 2k Consortium, 2013). Aridity at this time was only interrupted by a short relatively humid interval at around 1100 CE that could have been related with the Oort solar minimum, perhaps triggering El Niño conditions and more precipitation in the area as suggested in previous studies (Cook et al., 2004, Mann et al., 2009). An alternative explanation to the increase in *P. edulis* at that time could be related to a decrease in temperature directly related to the Oort solar minimum, which has been shown to have forced climate (Moberg et al., 2005). Return to more El Niño and wetter conditions occurred during the Little Ice Age (LIA) in three ca. 200-yr-cycle steps related with the Wolf, Spörer and Maunder solar minima and wettest conditions were reached at ca. 1750 CE, agreeing with precipitation estimations in the area (Cook et al., 2004) and El Niño-3 SST reconstructions (Mann et al., 2009).

Following the ocean dynamical thermostat hypothesis (Clement et al., 1996) and the centennial-scale cyclical pattern in solar and related *P. edulis*-ENSO precipitation shown in this study, a general trend towards La Niña conditions is observed since the LIA wet period until present, with a multidecadal-scale drought recorded at ca. 1850 CE, and related with the solar modern maximum (Reimer et al., 2020, Fig. 4). Our modern climate analog results (Fig. S6) provide a linkage between climatic processes and long-term SST conditions that support prolonged drought during persistent La Niña conditions resulting in reduced growth or die-off of *P. edulis* in the region. This is consistent with regional impacts of long-term persistent ENSO conditions impacting paleoevironmental records climatically and hydrologically (Brunelle et al., 2018). The combined result of a multidecadal-scale megadrought and associated climate processes, in the context of present anthropogenic global warming, similar or even more acute than during the MCA, will cause enhanced moisture stress and drastic and extensive forest die-off, associated land surface environmental changes, which will have major implications for ecosystems and ecosystem services in arid environments (Woodhouse, 2003, Cook et al., 2007, Calder et al., 2015). However, further investigations need to be performed in this respect as climate models suggest that ENSO teleconnections will change and the thermostat hypothesis may not apply because of a change in the mean state of the atmospheric circulation due to anthropogenic forcing such as greenhouse global warming (Yeh et al., 2018), likely producing an increase in the frequency of ENSO extremes (Cai et al., 2015).

CRediT authorship contribution statement

G. Jiménez-Moreno conceived the study, performed the analyses and wrote the paper. R.S. Anderson contributed with the idea and data. J.J. Shinker performed the modern climate analog analyses. All authors contributed to the interpretation, discussed the results and provided inputs to the paper.

Declaration of competing interest

The authors declare that they have no known competing financial interests or personal relationships that could have appeared to influence the work reported in this paper.

Acknowledgements

This study was supported by the project P11-RNM 7332 of the "Junta de Andalucía", the projects CGL2013-47038-R and CGL2017-85415-R of the "Ministerio de Economía y Competitividad of Spain and Fondo Europeo de Desarrollo Regional FEDER" and the research group RNM0190 (Junta de Andalucía). We thank Julio Betancourt for thoughtful comments on a previous version of the manuscript and Frank Sirocko and Guillaume Leduc for providing 106KL and M772-059 data. This paper benefited from the thoughtful comments and suggestions of two anonymous reviewers.

Appendix A. Supplementary material

Supplementary material related to this article can be found online at https://doi.org/10.1016/j.epsl.2021.117217.

References

Allen, C.D., Breshears, D.D., 1998. Drought-induced shift of a forest–Woodland ecotone: rapid landscape response to climate variation. Proc. Natl. Acad. Sci. USA 95, 14839–14842.

Anderson, R.S., 1993. A 35,000 year vegetation and climate history from Potato Lake, Mogollon Rim, Arizona. Quat. Res. 40, 351–359.

Anderson, R.S., Feiler, E., 2009. Holocene vegetation and climate change on the Colorado Great Plains, USA, and the invasion of Colorado piñon (*Pinus edulis*). J. Biogeogr. 36, 2279–2289.

Arriaga-Ramírez, S., Cavazos, T., 2010. Regional trends of daily precipitation indices in northwest Mexico and southwest United States. J. Geophys. Res. 115, D14111.

Asmerom, Y., Polyak, V., Burns, S., Rassmussen, J., 2007. Solar forcing of Holocene climate: new insights from a speleothem record, southwestern United States. Geology 35, 1–4.

Barron, J.A., Anderson, L., 2011. Enhanced Late Holocene ENSO/PDO expression along the margins of the Eastern North Pacific. Quat. Int. 235, 3–12.

Betancourt, J.L., Schuster, W.S., Mitton, J.B., Anderson, R.S., 1991. Fossil and genetic history of a pinyon pine (Pinus edulis) isolate. Ecology 72, 1685–1697.

Bond, G., et al., 2001. Persistent solar influence on north Atlantic climate during the Holocene. Science 294, 2130–2136.

Breshears, D.D., et al., 2005. Regional vegetation die-off in response to global-change-type drought. Proc. Natl. Acad. Sci. USA 102, 15144–15148.

Brunelle, A., Minckley, T.A., Shinker, J.J., Heyer, J., 2018. Filling a geographical gap: new paleoecological reconstructions from the desert Southwest, USA. Front. Earth Sci. 6, 106.

Cai, W., Santoso, A., Wang, G., Yeh, S.-W., An, S.-I., Cobb, K.M., Collins, M., Guilyardi, E., Jin, F.-F., Kug, J.-S., Lengaigne, M., McPhaden, M.J., Takahashi, K., Timmerman, A., Vecchi, G., Watanabe, M., Wu, L., 2015. ENSO and greenhouse warming. Nat. Clim. Change 5, 849–859.

Calder, J., Stopka, C., Parker, D., Jiménez-Moreno, G., Shuman, B.N., 2015. Medieval warming initiated exceptionally large wildfire outbreaks in the Rocky Mountains. Proc. Natl. Acad. Sci. 112, 13261–13266.

Cane, M.A., 2005. The evolution of El Niño, past and future. Earth Planet. Sci. Lett. 230, 227–240.

Carter, V.A., et al., 2018a. A 1,500-year synthesis of wildfire activity stratified by elevation from the US Rocky Mountains. Quat. Int. 488, 107–119.

Carter, V.A., Shinker, J.J., Preece, J., 2018b. Drought and vegetation change in the central Rocky Mountains and western Great Plains: potential climatic mechanisms associated with megadrought conditions at 4200 cal yrBP. Clim. Past 14, 1195–1212.

Clement, A.C., Seager, R., Cane, M.A., Zebiak, S.E., 1996. An ocean dynamical thermostat. J. Climate 9, 2190–2196.

Clement, A., Seager, R., Cane, M., 2000. Suppression of El Niño during the Mid-Holocene by changes in the Earth's orbit. Paleoceanography 15, 731–737.

Clifford, M.J., et al., 2013. Precipitation thresholds and drought-induced tree die-off: insights from patterns of Pinus edulis mortality along an environmental stress gradient. New Phytol. 200, 413–421.

Cole, K.L., et al., 2008. Geographical and climatic limits of needle types of one- and two-needled pinyon pines. J. Biogeogr. 35, 257–269.

Conroy, J.L., et al., 2008. Holocene changes in eastern tropical Pacific climate inferred from a Galápagos lake sediment record. Quat. Sci. Rev. 27 (11–12), 1166–1180.

Conroy, J.L., Overpeck, J.T., Cole, J.E., Steinitz-Kannan, M., 2009. Variable oceanic influences on western North American drought over the last 1200 years. Geophys. Res. Lett. 36, L17703.

Cook, E.R., Woodhouse, C.A., Eakin, C.M., Meko, D.M., Stahle, D.W., 2004. Long-term aridity changes in the western United States. Science 306, 1015–1018.

Cook, E.R., Seager, R., Cane, M.A., Stahle, D.W., 2007. North American drought: reconstructions, causes, and consequences. Earth-Sci. Rev. 81 (1–2), 93–134.

Debret, M., et al., 2009. Evidence from wavelet analysis for a mid-Holocene transition in global climate forcing. Quat. Sci. Rev. 28, 2675–2688.

Edwards, M.E., Mock, C.J., Finney, B.P., Barber, V.A., Bartlein, P.J., 2001. Potential analogues for paleoclimatic variations in eastern interior Alaska during the past 14,000 yr: atmospheric circulation controls of regional temperature and moisture responses. Quat. Sci. Rev. 20, 189–202.

Emile-Geay, J., Cobb, K., Mann, M., Wittenberg, A.T., 2013. Estimating central equatorial Pacific SST variability over the past millennium, part 2: reconstructions and implications. J. Climate 26, 2329–2352.

Emile-Geay, J., Cobb, K.M., Cole, J.E., Elliot, M., Zhu, F., 2021. In: McPhaden, M.J., Santoso, A., Cai, W. (Eds.), El Niño Southern Oscillation in a Changing Climate, first edition. In: Geophysical Monograph Series, vol. 253. American Geophysical Union, John Wiley & Sons, Inc.

Haug, H.G., et al., 2001. Southward migration of the Intertropical Convergence Zone through the Holocene. Science 293, 1304–1308.

Heyer, J.P., Brewer, S.C., Shinker, J.J., 2017. Using high-resolution reanalysis data to explore localized Western North America hydroclimate relationships with ENSO. J. Climate 30, 5395–5417.

Jiménez-Moreno, G., Anderson, R.S., 2012. Pollen and macrofossil evidence of Late Pleistocene and Holocene treeline fluctuations from an alpine lake in Colorado, USA. Holocene 23 (1), 68–77.

Jiménez-Moreno, G., Anderson, R.S., Shuman, B.N., Yackulic, E., 2019. Forest and lake dynamics in response to temperature, North American monsoon and ENSO variability during the Holocene in Colorado (USA). Quat. Sci. Rev. 211, 59–72.

Johnson, B.G., Jiménez-Moreno, G., Eppes, M.C., Diemer, J.A., Stone, J.R., 2013. A multiproxy record of postglacial climate variability from a shallowing, 12-m deep sub-alpine bog in the southeastern San Juan Mountains of Colorado, USA. Holocene 23, 1028–1038.

Koutavas, A., deMenocal, P.B., Olive, G.C., Lynch-Stieglitz, J., 2006. Mid-Holocene El Niño-Southern Oscillation (ENSO) attenuation revealed by individual foraminifera in eastern tropical Pacific sediments. Geology 34, 993–996.
Koutavas, A., Joanides, S., 2012. El Niño–Southern Oscillation extrema in the Holocene and Last Glacial Maximum. Paleoceanography 27, PA4208.
Lamy, F., Hebbeln, D., Rohl, U., Wefer, G., 2001. Holocene rainfall variability in southern Chile: a marine record of latitudinal shifts of the Southern Westerlies. Earth Planet. Sci. Lett. 185, 369–382.
Laskar, J., et al., 2004. A long term numerical solution for the insolation quantities of the Earth. Astron. Astrophys. Nor. 428, 261–285.
Liu, Z., et al., 2014. Evolution and forcing mechanisms of El Niño over the past 21,000 years. Nature 515, 550–553.
Loubere, P., Creamer, W., Haas, J., 2013. Evolution of the El Nino-Southern Oscillation in the late Holocene and insolation driven change in the tropical annual SST cycle. Glob. Planet. Change 100, 129–144.
Mann, M.E., et al., 2009. Global signatures and dynamical origins of the Little Ice Age and Medieval Climate Anomaly. Science 326, 1256–1260.
Meehl, G.A., Arblaster, J.M., Matthes, K., Sassi, F., van Loon, H., 2009. Amplifying the Pacific climate system response to a small 11-year solar cycle forcing. Science 325, 1114–1118.
Mesinger, F., et al., 2006. North American regional analysis. Bull. Am. Meteorol. Soc. 87, 343–360.
Moberg, A., Sonechkin, D.M., Holmgren, K., Datsenko, N.M., Karlén, W., 2005. Highly variable Northern Hemisphere temperatures reconstructed from low and high-resolution proxy data. Nature 433, 613–617.
Mock, C.J., 1996. Climatic controls and spatial variations of precipitation in the western United States. J. Climate 9, 1111–1125.
Mock, C.J., Brunelle-Daines, A.R., 1999. A modern analogue of western United States summer paleoclimate at 6,000 years before Present. Holocene 9, 541–545.
Mock, C.J., Shinker, J.J., 2013. Modern analog approaches in paleoclimatology. In: Elias, S.A. (Ed.), The Encyclopedia of Quaternary Science. Elsevier, pp. 102–112.
Mollier-Vogel, E., Leduc, G., Böschen, T., Martinez, P., Schneider, R.R., 2013. Rainfall response to orbital and millennial forcing in northern Peru over the last 18 ka. Quat. Sci. Rev. 76, 29–38.
Otto-Bliesner, B.L., Brady, E.C., Fasullo, J., Jahn, A., Landrum, L., Stevenson, S., Rosenbloom, N., Mai, A., Strand, G., 2016. Climate variability and change since 850 CE: an ensemble approach with the community Earth system model. Bull. Am. Meteorol. Soc. 97 (5), 735–754.
Pages 2k Consortium, 2013. Continental-scale temperature variability during the past two millennia. Nat. Geosci. 6, 339–346.
Power, M.J., et al., 2008. Changes in fire regimes since the Last Glacial Maximum: an assessment based on a global synthesis and analysis of charcoal data. Clim. Dyn. 30, 887–907.
Reimer, P.J., et al., 2020. IntCal20 northern hemisphere radiocarbon age calibration curve (0-55 cal kBP). Radiocarbon 62 (4), 725–757.
Rein, B., et al., 2005. El Niño variability off Peru during the last 20,000 years. Paleoceanography 20, PA4003.
Rodó, X., Rodriguez-Arias, M.A., 2004. El Niño–Southern oscillation: absent in the early Holocene? J. Climate 17 (3), 423–426.
Shinker, J.J., Bartlein, P.J., 2009. Visualizing the large-scale patterns of ENSO-related climate anomalies in North America. Earth Interact. 13 (3), 1–50.
Shinker, J.J., Bartlein, P.J., 2010. Spatial variations of effective moisture in the western United States. Geophys. Res. Lett. 37 (2).
Shinker, J.J., Bartlein, P.J., Shuman, B., 2006. Synoptic and dynamic climate controls of North American mid-continental aridity. Quat. Sci. Rev. 25, 1401–1417.
Shinker, J.J., 2014. Climatic controls of hydrologic extremes in south-interior intermountain west of Colorado, U.S.A. Rocky Mt. Geol. 49 (1), 51–60.
Shuman, B.N., Marsisek, J., 2016. The structure of Holocene climate change in mid-latitude North America. Quat. Sci. Rev. 141, 38–51.
Sulca, J., Takahashi, K., Espinoza, J.-C., Vuille, M., Lavado-Casimiro, W., 2018. Impacts of different ENSO flavors and tropical Pacific convection variability (ITCZ, SPCZ) on austral summer rainfall in South America, with a focus on Peru. Int. J. Climatol. 38, 420–435.
Swetnam, T.W., Betancourt, J.L., 1998. Mesoscale disturbance and ecological response to decadal climatic variability in the American Southwest. Clim. Change 11, 3128–3147.
Taschetto, A.S., Ummenhofer, C.C., Stuecker, M.F., Dommenget, D., Ashok, K., Rodrigues, R.R., Yeh, S.-W., 2021. In: McPhaden, M.J., Santoso, A., Cai, W. (Eds.), El Niño Southern Oscillation in a Changing Climate. In: Geophysical Monograph Series, vol. 253. American Geophysical Union, John Wiley & Sons, Inc.
Wise, E.K., 2010. Spatiotemporal variability of the precipitation dipole transition zone in the northwestern United States. Geophys. Res. Lett. 37, L07706.
Woodhouse, C.A., 2003. A 431-yr reconstruction of western Colorado snowpack from tree rings. J. Climate 16, 1551–1561.
Yeh, S.-W., Cai, W., Min, S.-K., McPhaden, M.J., Dommenget, D., Dewitte, B., Collins, M., Ashok, K., An, S.-I., Yim, B.-Y., Kug, J.-S., 2018. ENSO atmospheric teleconnections and their response to greenhouse gas forcing. Rev. Geophys. 56, 185–206.